



NRL - Contract - Reporting information for the months of August, September, October, November, December 1993 and January 1994.

## LOW VOLTAGE ELECTRON BEAM LITHOGRAPHY

Aaron Baum and R. Fabian Pease

DTIC  
ELECTE  
FEB 8 1994  
S C D

In order to develop a low-energy-spread, high brightness electron source using negative electron affinity technology, it is necessary to survey the effects of cathode structure and activation on energy spread, lateral velocity distribution, peak current, and lifetime. Most research in NEAPC technology has gone into detector applications, to improve photoyield at low light intensity and high wavelength. Intevac is a leader in this area. The scientific understanding and technical expertise developed in this effort are important to achieving our goal of an electron source optimized for low-energy electron applications; however, it will be necessary to investigate other cathode properties (peak brightness, energy spread) under a substantially different operating regime (high light intensity, small emission area, high extraction field).

To this end it is important to examine the operation of the photocathode in detail; the best way to describe this is by tracking the life of an electron, illustrated in Figure 1. We start with an electron in the valence band (step 1), which is excited by an incoming photon into the conduction band (step 2). The electron then relaxes, by optical phonon scattering (which has a mean free path of about 300A), into the conduction band minimum, where the electron has a fairly long lifetime, which leads to a long diffusion length (a few  $\mu\text{m}$  in a good photocathode). Thus electrons excited within a few  $\mu\text{m}$  of the surface have a high probability of reaching the surface. It should be noted here that Intevac has developed the technology of a glass-bonded thin film photocathode which can be used in transmission mode (light entering from beneath the surface). Besides offering ruggedness and simplicity of electron gun design, transmission mode NEAPCs offer lower energy spread than the more commonly used reflection-mode NEAPCs. In reflection mode, there are many more "hot" electrons — electrons which haven't yet thermalized to the CMB — at the surface; in reflection mode NEAPCs, many of these "hot" electrons escape, broadening the energy spread.

When the electrons reach the surface, they encounter the band-bending region, where they are accelerated toward the surface. Since the electrons are "hot" in this region, they may interact with optical phonons here and lose (or gain) energy (step 3). Thus their energy spread increases. Electrons with energy above the vacuum level can then escape. The work-function-lowering activation layer, by determining the vacuum level, acts as an energy filter, blocking the lower-energy electrons from escaping.

DISTRIBUTION STATEMENT A

Approved for public release  
Distribution Unlimited

94-04177

07 032

**Best  
Available  
Copy**

There is another phenomenon at the surface that plays a potentially important role in improving brightness of NEAPC sources. Because the electrons have appreciably lower effective mass in the semiconductor than in vacuum (a ratio of 1:15 for GaAs), their semiconductor quantum-mechanical wavelength is much shorter. When the electrons are emitted into vacuum, quantum-mechanical refraction takes place, and the electrons are focused into a narrow forward cone. This is an excellent property for an electron source.

The activation layer also plays a role in determining emission characteristics. In the layer, electrons may scatter elastically, which would degrade their angular distribution, or inelastically, which would degrade both their angular and energy distributions. This consideration favors a thinner activation layer.

To optimize the NEAPC source for low-energy electron beam work, we are examining the effect of activation layer thickness on both the lateral and total energy spreads. One structure being examined is a GaAsP cathode activated with only a monolayer of Cs. This type of NEAPC has not been fully investigated as it has lower quantum efficiency and less sensitivity to long wavelengths than currently used cathodes. However, the thin activating layer should minimize scattering, improving brightness, and an extremely low energy spread should be obtainable by adjusting the bandgap and using the vacuum level as an energy filter. Other possibilities include activation with F instead of O, which may provide thinner activation layers, and increasing the doping near the surface. The latter modification would decrease the width of the depletion region and thus improve the energy spread of emitted electrons as they will be less likely to scatter there.

Figure 2 shows a possible optimized photocathode structure. Like the typical Intevac cathodes, this structure uses AlGaAs to block electrons from diffusing too far from the surface; this design also incorporates a graded bandgap to accelerate the electrons toward the surface. This action improves the cathode's efficiency and decreases the cathode's response time (which is in the tens of picoseconds even without this improvement). Also, since a small source size is desirable from an electron optics standpoint, if the laser is focused to a diffraction-limited spot in the active region, the graded bandgap will reduce the diffusive spreading of the electrons before emission. To further improve the source size and response time of the cathode, it is designed to be thinner than an ordinary cathode, perhaps less than 1 micron. The most important modifications, however, are near the surface. The depletion region has been reduced by "spike doping," — the last 100 Å of the cathode are doped as heavily as possible. Furthermore, a thin Cs-only activation layer is employed. These modifications should greatly reduce scattering in these two regions, improving energy spread and brightness.

Currently we are examining the effect of activation on cathode brightness. The experiments are carried out using photocathodes made using Intevac's proprietary techniques sealed in tubes at UHV. Our first series of measurements consists of measuring the lateral energy distributions of electrons emitted from various photocathodes by monitoring the current intercepted by a knife edge that is transported across the beam. The tube design is shown in Figure 2. This apparatus affords the highest resolution measurements of this type ever made on negative electron affinity devices. Initial measurements have been made on photocathodes activated with the standard Intevac nightvision activation, and show that, as expected, the electrons have very low lateral velocities, corresponding to approximately 40meV on average. Tubes with GaAsP cathodes and Cs-only activations are being fabricated.

Future experiments will involve measuring total energy spread, lifetime, and peak brightness of a variety of cathode structures.

DTIC QUALITY INSPECTED 6

Accession For	
NTIS CRA&I	<input checked="" type="checkbox"/>
DTIC TAB	<input type="checkbox"/>
Unannounced	<input type="checkbox"/>
Justification	
By <i>Per A263360</i>	
Distribution /	
Availability Codes	
Dist	Avail and/or Special
<i>A-1</i>	

# Fig. 1. Negative Electron Affinity Photoemission

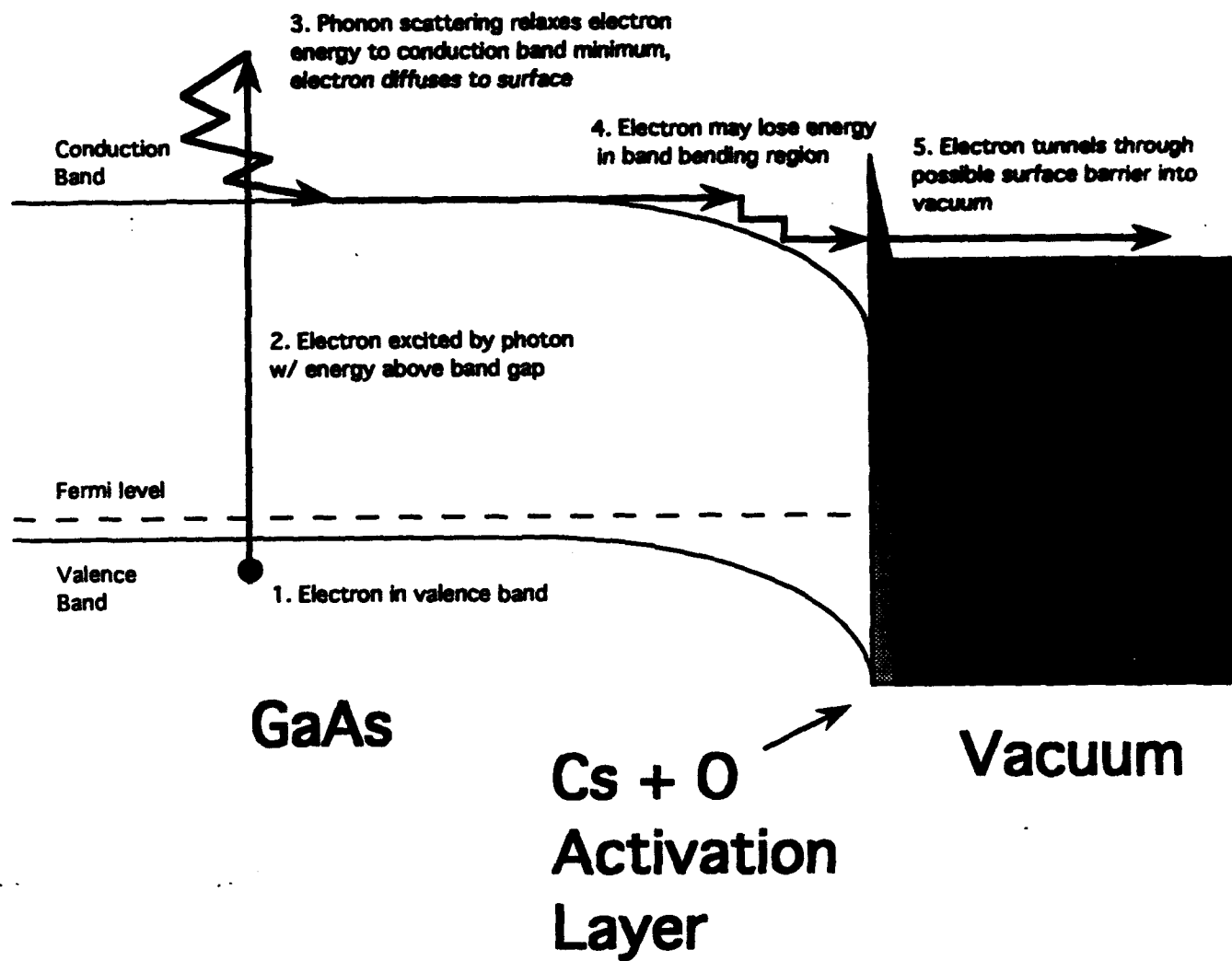
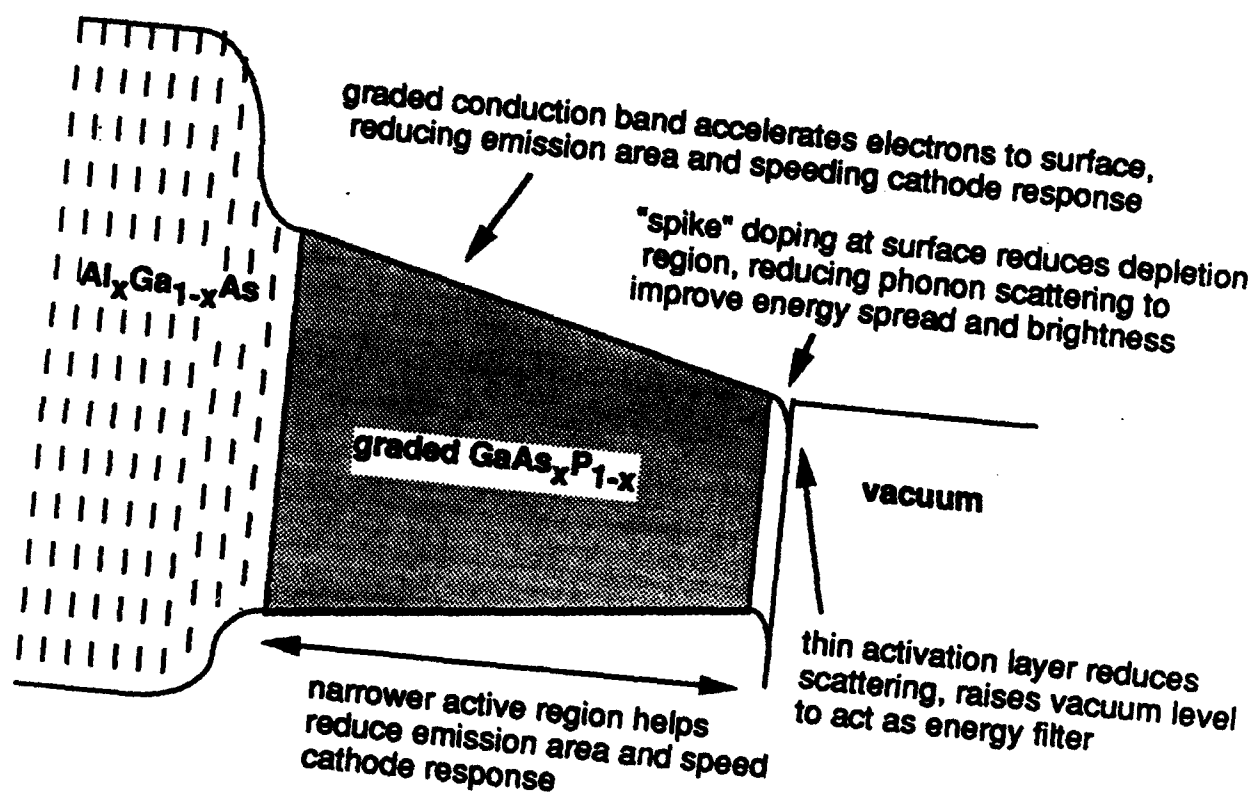


**Fig. 2. Band Diagram of Possible Optimized Photocathode Structure**



# **FIRST DRAFT**

## **Current Status of Computer Models for Charged Particle Systems**

**Brent Boyer and R. F. W. Pease**

*Although there are many analytical methods available for analyzing charged particle systems, in general they apply to geometrically simple lens systems. As a result, computer modeling has emerged as a powerful tool for designing systems which will extract, focus, and analyze charged particle beams. Personal computers are now sufficiently powerful and economical that any researcher can have access to the necessary computer resources. This has caused computer modeling to become very popular. Here we summarize the main features of computer modeling for charged particle systems. The topics covered include numerical techniques, source modeling, lens design, deflector modeling, tolerances, space charge effects, and beam-target interactions.*

### **Introduction**

Although the earlier textbooks on electron (and ion) optics antedated the widespread use of computers, the use of computers for solving electron optical problems goes back at least four decades. During the early fifties Liebmann and his colleagues at the AEI Research Centre in the UK employed a combination of resistance network analog computation and digital integration to solve for fields and published a series of papers that became the 'bible' for those designing axially symmetric electrostatic and magnetic lenses [1]. Munro in 1970 described a series of programs for doing the same calculations on a 'modern' digital computer far more rapidly and conveniently [2]. His results bore out those of the AEI team almost exactly.

For analyzing such lenses the first task is solve the Laplace equation according to the boundary conditions set by the magnetic polepieces and their magneto-static potentials, and by the electrodes and their electric potentials. For axial symmetry and with no polepieces or electrodes on axis (the usual arrangement) the properties of the solutions to the Laplace equation are such that it is possible to determine both first order properties (focal lengths, principal plane positions and chromatic aberration coefficient) and third order properties (e.g. spherical aberration) of the resulting lenses from only the on-axis distributions of electric and magnetostatic potentials,  $V(0,z)$  and  $\Phi(0,z)$ . A worked example for a magnetic lens is shown below in the section on Lens Modeling using a series of programs written by Munro. Munro's programs can also be used to determine the magnetostatic potential when the material in the magnetic circuit approaches saturation.

The limitation of the above treatment is that it does not take into account higher order aberrations (5th order and above) which may be significant for certain cases. To do a precise simulation of charged particle optics requires determination of the fields everywhere, not just on-axis, and the particle trajectories are determined by numerical integration of the corresponding equation of motion. The techniques for calculating fields - both on-axis and everywhere - along with numerical ray tracing are discussed below in the section on Numerical Techniques.

Another issue in charged particle optics are those mutually repulsive forces that charged particles exert between themselves. This effect is known as space charge and it has deleterious effects on beam quality. Traditionally, the beam perveance,  $IV^{-3/2}$ , was a parameter used to indicate how seriously space charge will affect the beam quality. If the perveance was sufficiently low then the space charge effect was thought to be negligible. This was the result from work done on vacuum tubes where the space charge was modeled as a continuum of charge density; this model predicts that space charge acts as a diverging lens. In most electron beam lithography equipment the values of perveance are such that this lens effect is negligible and so space charge was ignored until about 1970 in this application. However, it has since been established that in such equipment the occurrence of random interactions is sufficiently frequent to cause surprisingly large energy spread (the 'Boersch effect') and appreciable trajectory bending [3]. Because of the random nature of these interactions this phenomenon is best treated using a Monte Carlo technique in which the position and momentum of each of a finite population of particles is tracked as the particles move down the column [4]. A whole section below is devoted to modeling the space charge effect.

Electron sources for electron beam lithography equipment traditionally have been relatively simple structures [5]. However point sources for both ions and electrons pose challenges for modelling because of the huge disparity between the nm-scale geometries of the tips and the cm-scale geometries of the surrounding electrodes. How this is presently tackled is described in the section on Source Modeling, but it is not clear that a satisfactory approach yet exists.

Finally, the interaction of the beam with the solid target can be modeled as a continuous slowing down of the particles that suffer scattering at random intervals at a mean frequency set by scattering cross sections of the incident particles in the target material. Such modelling has been the subject of countless papers since 1963 and a brief description along with references to recent literature is given in the section on Beam-Target interactions.

## Numerical Techniques

With the exception of source modeling and space charge effects, much of the computing required for Charged Particle systems goes into determining electric and/or magnetic fields from boundary conditions such as potentials on electrodes or current through coils. This section will briefly describe some of the numerical techniques available for calculating these fields, and will conclude with a discussion of numerical ray tracing.

For a cylindrically symmetric system (no  $\phi$  dependence), any potential (electric or scalar magnetic) will have the following Taylor expansion since it satisfies the Laplace Equation [6]:

$$\Phi(r, z) = \Phi(z) - \frac{1}{4}\Phi''(z)r^2 + \frac{1}{64}\Phi''''(z)r^4 - \dots \quad (1)$$

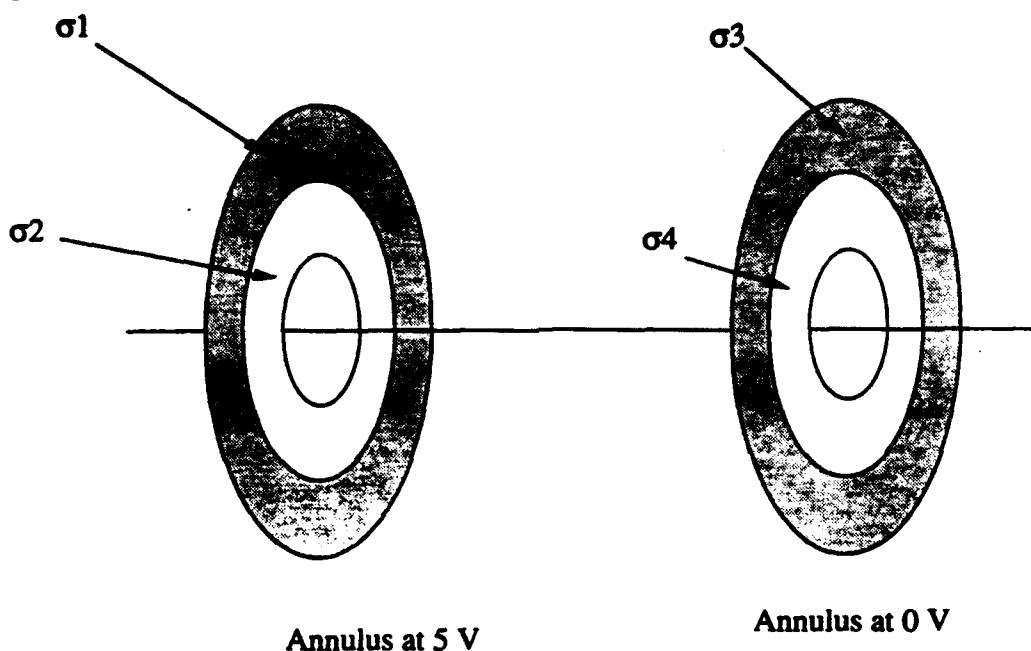
This says that the potential at any point  $(r, z)$  can be determined merely by knowing  $\Phi(r = 0, z)$ . So, in principle, you do not need to explicitly compute the potentials everywhere; you only need to compute them along the  $z$ -axis.

Although the above Taylor expansion will only be valid for small values of  $r$ , much useful information may still be extracted. For example, the paraxial ray equation and third order aberration theory can be derived from it. See the references in [7] for more details. In addition, a modified form of equation (1) is used when designing deflectors, as will be discussed below.

It also may happen that one needs the full solution to the potential/field everywhere inside the system, not just near the optical axis. This will be required, for instance, to do full ray tracing of particles down the column and especially to do ray tracing near an electron gun. In this case, the full partial differential equation (Laplace's equation) must be solved.

Discussed below are the three most popular techniques for solving for potentials, either on-axis or everywhere inside the system. These methods are the boundary element method (BEM), the finite difference method (FDM), and the finite element method (FEM).

The boundary element method, also known as the charge-density method, is one way to quickly determine  $\Phi(r, z)$  for electrostatic problems. What one does is to break up the electrodes into smaller elements (e.g. an annulus might be broken up into sections of rings) and then determine what charge density must be uniformly distributed throughout each element in order to give rise to the prescribed potentials on all boundary elements. Here is an example:



This determination of the charge density will involve solving a matrix equation. The potential at any point in space due to a single element is then simply found by using the formula

$$\Phi_i = \frac{1}{4\pi\epsilon_0} \iiint dV \frac{\rho}{r} \quad (2)$$

Note that the charge density  $\rho$  is uniform, so it may be pulled out of the volume integral; typically the shapes used for the boundary elements are such that analytic expressions exist for the remaining volume integral. The total potential at any point in space is then the sum of the potentials from all elements. Consult the references in [8] for more details.

The finite difference method is very simple to understand. Recall that the interpretation of the first derivative of a curve is that it is the slope of the tangent line at that point. If a curve  $c(x)$  is sampled at a finite number of points, say a grid of points equally spaced by the distance  $\Delta x$ , then we might approximate the first derivative of  $c(x)$  by

$$\left. \frac{dc(x)}{dx} \right|_{x=a} \approx \frac{c(a + \Delta x) - c(a)}{\Delta x} \quad (3)$$

Similarly, the second derivative may be approximated by

$$\left. \frac{d^2 c(x)}{dx^2} \right|_{x=a} \approx \frac{c(a + \Delta x) - 2c(a) + c(a - \Delta x)}{\Delta x^2} \quad (4)$$

Similar formulas hold for partial derivatives. Then any second order PDE with boundary conditions should be solvable as follows: lay out a mesh of grid points with the appropriate dimensionality (say a rectangular grid aligned with the  $x$  and  $y$  axis for a 2D problem) and insist that the PDE (as expressed with the above approximations) be satisfied at every interior mesh point, and the boundary conditions be satisfied at every boundary mesh point. This will generate a set of simultaneous, linear, algebraic equations (i.e. a matrix equation) which can be solved yielding the potential everywhere.

The finite element method is less intuitive. It turns out that solutions of PDEs are also solutions of an associated variational problem. What is important is that finite element methods are similar to finite difference methods in that one must specify a grid of points. One also must specify how the solution is assumed to vary over a given mesh surface element; a first order FEM assumes the solution is piecewise linear while a second order solution assumes the solution is piecewise quadratic. Finite element methods are more general than finite difference methods (indeed, FDM can be shown to be a subcase of FEM). One consequence of this is that FEM can be easily applied to nonrectangular meshes; triangular meshes are very common. This may be a large advantage in accuracy when the boundary is very nonrectangular - triangular meshes can easily be chosen to have the boundary mesh sides lie closely along the boundary [9]. Rectangular meshes suffer in that their boundary mesh sides often weave through a rough boundary instead of lie along it. In addition, FEM is the only way to handle saturated magnetic lenses. Standard algorithms like Gaussian elimination may be completely inadequate for solving the huge matrix equation generated by FEM (e.g. solving Poisson's equation using second order FEM). Workers in the field have now begun to employ the incomplete Choleski conjugate gradient (ICCG) method [10] and report considerable success with it - see [11] and [12].

For more details concerning FDM and FEM, a modern reference is Hall and Porsching[13]; consult pp.159-183 of Hawkes [9] for the application of these methods to charged particle optics. Other references to the application of FEM for solving electrostatic fields may be found in [14].

To compare BEM with FEM for solving an electrostatic problem, note that with BEM you only break up the electrodes into small pieces whereas with FEM the whole space is broken into grid elements. This means that the size of the matrix equation which must be solved for a BEM solution is significantly smaller than that for FEM, which is a significant advantage for the BEM method. On the other hand, with FEM, once you have solved the matrix equation you have the solution for the potential everywhere whereas BEM only yields the charges on the electrodes. To get the potential at a given point from a BEM solution you must add up the potentials due to the charge on each boundary element; this may be a modest computation as the geometrical integral from equation (2) may be, say, an elliptic integral if the boundary element is a ring (Reneau, [8]). So, if there are many boundary elements or if you are ray tracing a sufficiently large number of particles, the FEM may be more economical. One exception may be ray tracing using the paraxial ray equation. In this case, since you only need the potential on-axis, the BEM may be more economical.

Given the solution for the potential, one must still extract the fields if one desires to perform numerical ray tracing. Since the field is the gradient of the potential, this means that you must have the spatial partial derivatives of the potential. If a grid technique like FEM has been used, the potential is only known on the grid nodes which means that an accurate method for smooth interpolation between nodes must be developed. Chapter 13 of Hawkes [9] goes into detail describing some of the available methods; see also some of the references in [14]. Lunney *et al* [15] have developed a new method based on multipole expansion which they claim is a superior alternative to interpolation based schemes for computing the field.

Once the fields have been determined, an accurate method for ray tracing the particles must be employed. If a cylindrically symmetric system is under consideration and one has solved for the axial field, then one may elect to solve for the trajectories using the paraxial ray equation [7]. For a magnetic lens system, the paraxial ray equation is

$$\frac{d^2 r(z)}{dz^2} + \frac{\eta}{8V_r} B(z)^2 r(z) = 0 \quad (5)$$

where  $\eta$  is the charge to mass ratio and  $V_r$  is the relativistically corrected beam voltage. It is just an ordinary differential equation for the radial coordinate of the trajectory as a function of the axial coordinate, so the standard methods such as Runge-Kutta or Predictor-Corrector may be employed to numerically solve it. See Press *et al* for a good description of these techniques [16].

If the accuracy of the paraxial ray equation is insufficient, then more precise techniques must be employed. One such accurate way of ray tracing is to consider a Taylor series expansion in order to determine the future position of a particle given its present position:

$$\mathbf{r}(t + \Delta t) = \mathbf{r}(t) + \mathbf{r}'(t)\Delta t + \frac{1}{2}\mathbf{r}''(t)\Delta t^2 + \frac{1}{6}\mathbf{r}'''(t)\Delta t^3 + \dots \quad (6)$$

where primes denote differentiation with respect to the time  $t$ . If  $\mathbf{v}(t)$  is defined as the velocity and  $\mathbf{a}(t)$  as the acceleration, we can rewrite equation (6) as:

$$\mathbf{r}(t + \Delta t) = \mathbf{r}(t) + \mathbf{v}(t)\Delta t + \frac{1}{2}\mathbf{a}(t)\Delta t^2 + \frac{1}{6}\mathbf{a}'(t)\Delta t^3 + \dots \quad (7)$$

Making use of Newton's Second law ( $\mathbf{F} = m\mathbf{a}$ ), we can express this as:

$$\begin{aligned} \mathbf{r}(t + \Delta t) = & \mathbf{r}(t) + \mathbf{v}(t)\Delta t + \frac{1}{2m}\mathbf{F}(\mathbf{r}(t), t)\Delta t^2 \\ & + \frac{1}{6m}\left[(\mathbf{v}(t) \cdot \nabla)\mathbf{F}(\mathbf{r}(t), t) + \frac{\partial \mathbf{F}(\mathbf{r}(t), t)}{\partial t}\right]\Delta t^3 + \dots \end{aligned} \quad (8)$$

The force  $\mathbf{F}$  for electromagnetic forces is

$$\mathbf{F}(\mathbf{r}(t), t) = q(\mathbf{E} + \mathbf{v} \times \mathbf{B}) \quad (9)$$

and is in general a function both of particle position and time since  $\mathbf{E}$ ,  $\mathbf{v}$ , and  $\mathbf{B}$  in general depend on position and time. From equation (8) you can trace the particles' trajectory by advancing the time in small increments  $\Delta t$ . This is known as the power series method of ray tracing. The terms shown in equation (8) constitute a third order power series method; it is common to drop the last term and do a second order method if less accuracy will suffice.

An alternative to the power series approach would be to numerically solve the differential equation for the trajectory. This differential equation is just Newton's Second Law:

$$\frac{d^2\mathbf{r}(t)}{dt^2} = \frac{1}{m}\mathbf{F}(\mathbf{r}(t), t) \quad (10)$$

where  $\mathbf{F}$  is again given by equation (9). It is simple to see that in rectangular coordinates, this equation breaks down into three coupled ordinary differential equations. Then the standard techniques like Runge-Kutta or Predictor-Corrector may be used to solve them [16]; see [17] as an example in the literature where this is applied to charged particle trajectories.

A very accurate technique for tracking a particle's motion in a force field is the technique of Nystrom integrators, developed in 1925 by Nystrom [18]. This technique is also very complicated which has hindered its acceptance. Lear has exploited the capabilities of computers to ease the difficulty of implementing the method [19]. His application was actually the study of orbital motion, but perhaps there may be application in charged particle optics.

## Source Modeling

There are several issues involved in modeling charged particle sources. First, there must exist a good physical model for the emission process. For thermionic electron sources, the Richardson-Dushman equation with Schottky's field enhancement correction has proven to be a good model. Field emission electron sources are adequately modeled by the Fowler-Nordheim equation. A difficult source to model is liquid metal ion sources, because the tip is not fixed but changes shape during the emission process in a manner which is hard to predict.

Once the appropriate model has been selected, a source modeling program needs to very accurately determine the fields near the source. This is both because the emission process itself always strongly depends on the field configuration and also because the electrons will be ray traced upon emission. The most common candidates for determining the fields are the grid methods (FDM or FEM). In a typical electron source, the emission area may be as small as a few hundred angstroms while the extraction electrodes may be spaced millimeters away from the source. This huge length scale difference means that a grid method for solving the fields cannot have constant grid spacing - this would require too many elements to adequately model the source region. Thus, the grid must change scale from small grid spacing near the source to large grid spacing near the electrodes. This is almost always far too tedious for a human to specify the grid sizing by hand, so a good source modeling program should include a routine for automatically generating a grid with adaptive length scales.

Lastly, it is usually vital to include space charge effects when modeling the emission process - the repulsion caused by electrons which have already been emitted can greatly affect the emission of additional electrons. Furthermore, the presence of other electrons will modify the trajectories that would result if only fields from the electrodes were present. See below for a whole section which is devoted to techniques for modeling space charge effects.

One of the most comprehensive solutions to modeling electron sources is the program SOGUN reported by Zhu and Munro [12]. Their program can handle either thermionic or field emission guns. They use a 2nd order, isoparametric FEM code to solve for the electric potential. The sides of the grid elements in this technique are not lines but are quadratic curves - this enables the grid lines to almost perfectly conform to the boundary shapes (e.g. curved cathodes and electrodes). The fact that this is a 2nd order method means that the potential can be solved with higher accuracy. Once the potential has been solved for, the electric field needs to be extracted. This is one difficulty with isoparametric grids, but Zhu and Munro report a new algorithm to do this. The commercial version of this program, SOURCE, also includes automesh generation so that logarithmic changes in grid size - which is needed for field emission guns - can be done by computer [20]. Ray tracing is done by a third order power series method [21].

and space charge effects are modeled by iteratively solving Poisson's equation as discussed below. The program is able to determine the total beam current, the crossover position and size, and beam aberrations. Sample outputs from Munro's software may be found on the next two pages, where they model a thermionic  $\text{LaB}_6$  gun and a field emission gun.

Other earlier work on modeling sources may be found in Weber [22], Herrmannsfeldt [23], Kang [24], and Renau [25]. Browning [26] has successfully employed the BEM. See Hawkes [27] for a discussion of an analytical model for source region space charge effects. A reference to modeling liquid metal ion sources may be found in Cui and Tong [28]. Mohammed and Garcia [29] discuss automesh generation for electrostatic problems.

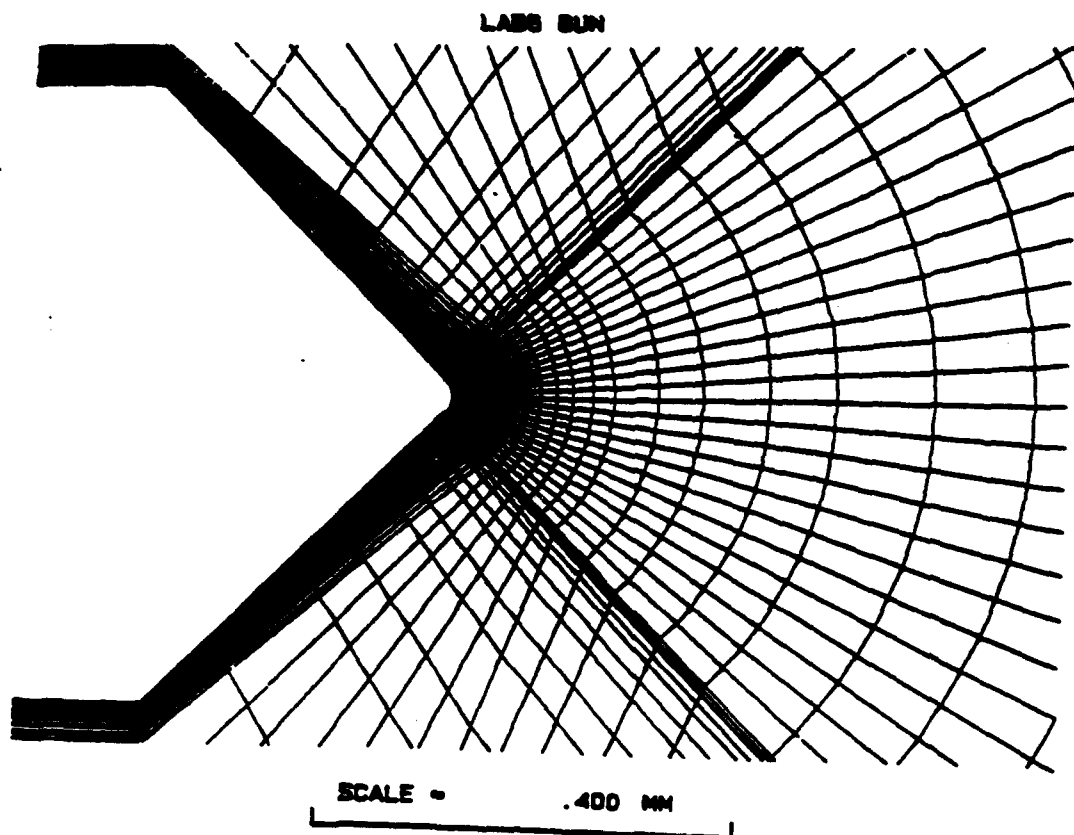


FIG. 7. Finite-element mesh layout in the cathode tip region of a LaB<sub>6</sub> gun.

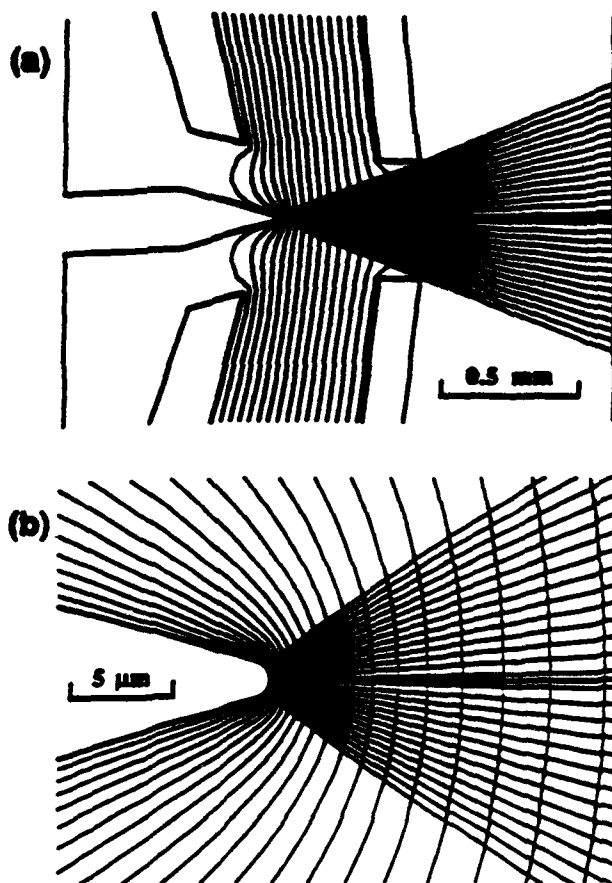


FIG. 8. Computed equipotentials and trajectories in as field emission gun.  
(a) Overall view. (b) Closeup view of field emission tip region.

## Lens Modeling

Lens modeling is the most well developed area for computer modeling of charged particle systems, with early programs appearing over 20 years ago [2].

The common feature of almost all probe forming lenses, whether electrostatic or magnetostatic, is that they have cylindrical symmetry. For example, a typical electrostatic lens consists of ring electrodes and a typical magnetostatic lens is cylindrical current coils surrounded by high permeability materials which concentrate the magnetic field across a small gap. This symmetry reduces a 3D field problem to a 2D problem.

The historical method of handling this problem is to consider a Taylor series expansion of the potential (Equation 1). This method requires knowledge of the potentials on-axis, which can be obtained by any of the means described in the Numerical Techniques section. Once these have been obtained, the on-axis fields (electric or magnetic) are easily determined and then the paraxial ray equation - an ordinary differential equation (see equation 5) - must be numerically solved for certain trajectories (the "principal rays"). These trajectories are then used in numerical integrations to obtain the aberration coefficients; important ones are spherical and chromatic aberrations. These aberration coefficients are then used to predict lens performance. Chu and Munro [7] report on a program capable of modeling both lenses and deflectors in this manner.

We give a worked example below of how to model the performance of a magnetic lens. This will give the reader an idea of what computer modeling of charged particle optics involves. This particular example is taken from a manual Munro has provided our lab [30].

### **Worked Example**

The lens geometry we will consider is shown on the next page, labeled as "Fig. 18b". The first task will be to determine the axial magnetic field (also known as the flux density), using Munro's program M11. Because of the symmetry of the lens, we need only solve over the region AYZD; this region is shown in detail in "Fig. 19b". M11 expects that you have divided the geometry into quadrilaterals, as shown in "Fig. 20b", in which edges of the pole piece lie along edges of the quadrilaterals. You will need to tell M11 the exact location of these quadrilaterals. Furthermore, since M11 uses a FEM technique to solve for the magnetic scalar potential everywhere inside AYZD, you will need to tell M11 what density of mesh lines to use inside each quadrilateral. This is sketched out in "Fig. 21b": the numbers along the lines YZ and ZD are the locations, in millimeters, of the corresponding quadrilateral vertex; the numbers along the lines AD and AY label the mesh lines thru the quadrilateral edges. The completed mesh is shown in "Fig. 22b". Now the steps outlined above are something that you the user do on paper - the actual input data supplied to the computer, in the form of a text file, is shown in "Table 1b". This is the format of "Table 1b": the first two big blocks of numbers are the axial ("z") and radial ("r") coordinates of the quadrilateral vertices; the numbers 1-7-12-22-27 and 1-5-10-15-20 on the top and left of these blocks are the mesh line labels (compare with "Fig. 21b"). The next line of numbers, 1-22-5-15-1000 tells the location of the pole piece and its relative permeability. The final two columns of numbers tell the boundary potential distribution (in ampturns). The output of this program is the axial magnetic field, shown in "Table 2b".

Now that the axial magnetic field has been obtained, we may go on to examine the objective properties of the lens. Munro's program M21 will calculate the excitation parameter and - depending on the magnification condition - the object and/or image plane, the objective principal plane, the objective focal length, the objective magnification, the spherical aberration coefficient, the chromatic aberration coefficient, and the magnetic field at the object and/or image plane. These are the main properties needed to predict lens performance. Along with the data file containing the axial magnetic field, the user must also input to M21 the initial beam voltage, the increment in beam voltage, the number of beam voltages, the magnification condition (zero, low, high, or infinite), and possibly the position of the object or image plane (if the magnification is either low or high). Examples of the output of M21 for the lens of "Fig. 18b" are found in "Table 14" and "Table 15".

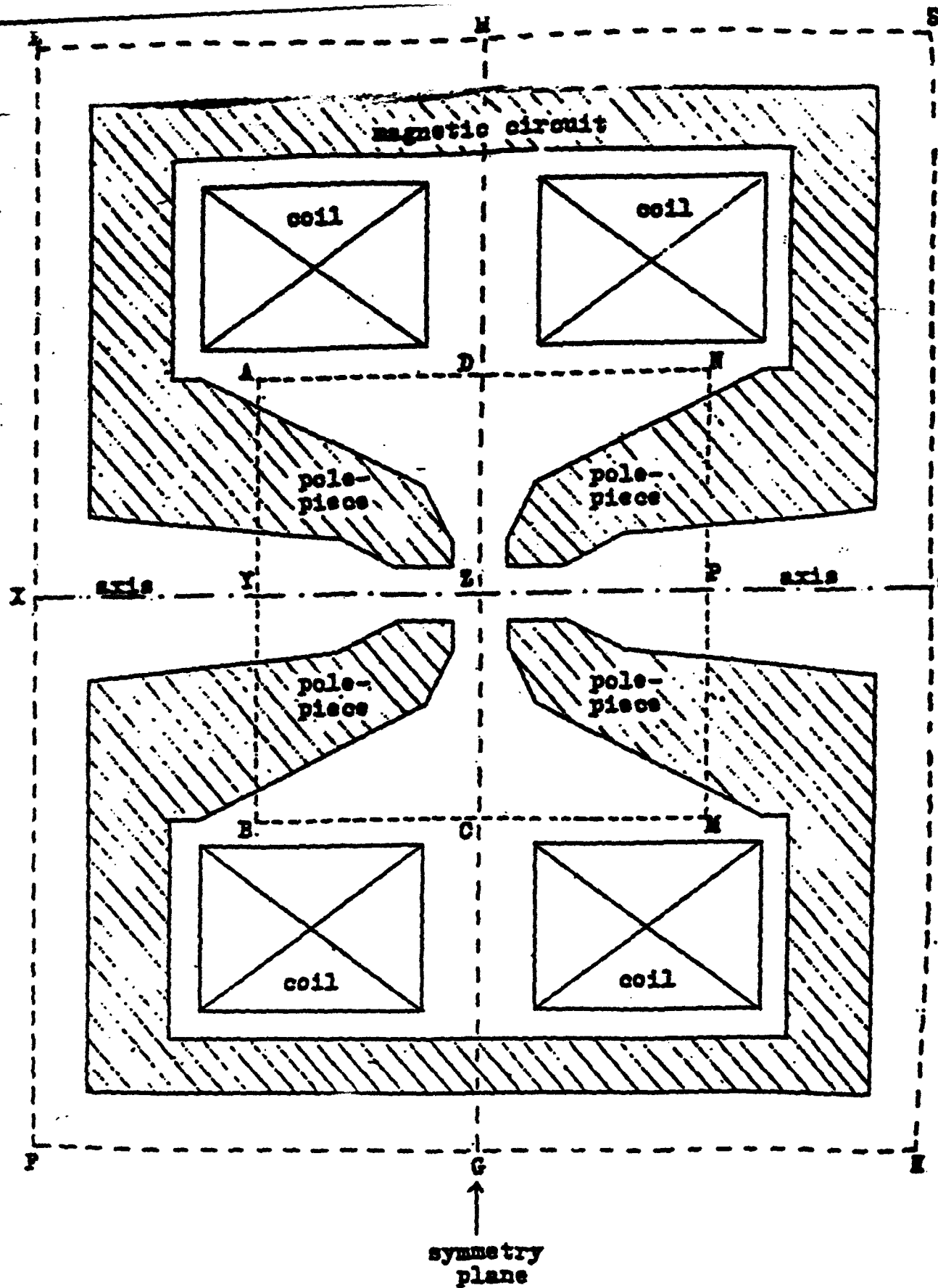


**Fig. 18b** Cross-section of a symmetrical magnetic lens

obj.  
side

Y axis Z

Fig. 19b

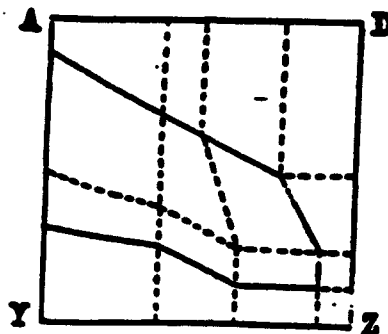


Fig. 20b

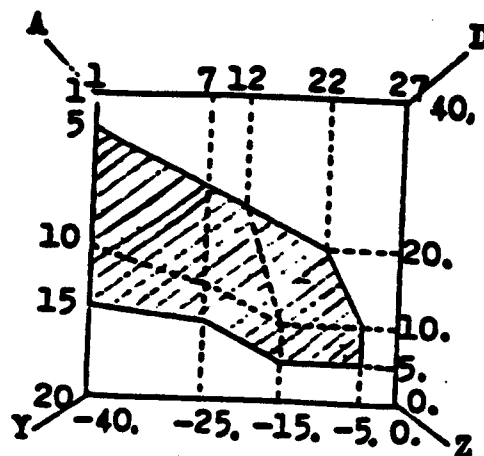


Fig. 21b

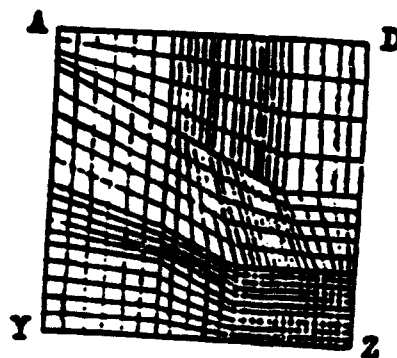


Fig. 22b

Table 1b   Sample data for Program M11 (data for the symmetrical pole-pieces of Fig. 18b)

POLE-PIECES OF FIG. 18B

	1	1			
	1	7	12	22	27
1	-40.	-25.	-20.	-10.	0.
5	-40.	-25.	-20.	-10.	0.
10	-40.	-25.	-15.	-5.	0.
15	-40.	-25.	-15.	-5.	0.
20	-40.	-25.	-15.	-5.	0.
	1	7	12	22	27
1	40.	40.	40.	40.	40.
5	35.	27.5	25.	20.	20.
10	20.	15.	10.	10.	10.
15	12.	10.	5.	5.	5.
20	0.	0.	0.	0.	0.
1	22	5	15	1000.	
1	-250.				
20	-250.				
1	-250.				
27	0.				
1	0.				
20	0.				

**Table 2b** Sample results for Program M11 (computed axial flux density distribution for the symmetrical pole-pieces of Fig. 18b)

**POLE-PIECES OF FIG. 18b**

**AXIAL FLUX DENSITY DISTRIBUTION**

<b>Z (MILLIMETRES)</b>	<b>B (TESLAS)</b>
-40.0000	0.000066
-37.5000	0.000066
-35.0000	0.000067
-32.5000	0.000068
-30.0000	0.000070
-27.5000	0.000073
-25.0000	0.000077
-23.0000	0.000084
-21.0000	0.000097
-19.0000	0.000136
-17.0000	0.000210
-15.0000	0.000517
-14.0000	0.000804
-13.0000	0.001223
-12.0000	0.001901
-11.0000	0.002966
-10.0000	0.004623
-9.0000	0.007154
-8.0000	0.010909
-7.0000	0.016231
-6.0000	0.023223
-5.0000	0.031372
-4.0000	0.039143
-3.0000	0.045156
-2.0000	0.049159
-1.0000	0.051377
0.0000	0.052081
1.0000	0.051377
2.0000	0.049159
3.0000	0.045156
4.0000	0.039143
5.0000	0.031372
6.0000	0.023223
7.0000	0.016231
8.0000	0.010909
9.0000	0.007154
10.0000	0.004623
11.0000	0.002966
12.0000	0.001901
13.0000	0.001223
14.0000	0.000804
15.0000	0.000517
17.0000	0.000210
19.0000	0.000136
21.0000	0.000097
23.0000	0.000084
25.0000	0.000077
27.5000	0.000073
30.0000	0.000070
32.5000	0.000068
35.0000	0.000067
37.5000	0.000066
40.0000	0.000066

500.00 AMPTURNS = LENS EXCITATION

**Table 14 Sample Data and Results for Program 121 (for zero magnification conditions)**

1000. 1000. 20 0

**OBJECTIVE PROPERTIES OF  
POLE-PIECES OF FIG. 18B  
FOR ZERO MAGNIFICATION CONDITIONS**

(THE ABERRATION COEFFICIENTS ARE REFERRED TO THE IMAGE SIDE)

RC BEAM VOLTAGE	EXCITATION PARAMETER	IMAGE PLANE	PRINC PLANE	FOCAL LENGTH	SPHER. AB.	CHROM. AB.	FIELD AT ZI
VR(VOLTS)	NI/SQRT(VR)	ZI(MM)	ZP(MM)	FO(MM)	CSI(MM)	CCI(MM)	(TESLAS)
1000.	15.81	1.88	-2.69	4.57	3.11	3.36	0.0495
2000.	11.18	4.67	-1.64	6.31	5.76	4.84	0.034
3000.	9.13	6.92	-1.10	8.02	9.78	6.41	0.0167
4000.	7.91	8.99	-0.80	9.79	15.90	8.10	0.0072
5000.	7.07	10.99	-0.63	11.62	24.63	9.88	0.0030
6000.	6.45	12.96	-0.51	13.47	36.44	11.71	0.0012
7000.	5.98	14.90	-0.43	15.33	51.82	13.56	0.0005
8000.	5.59	16.83	-0.38	17.21	71.26	15.42	0.0002
9000.	5.27	18.75	-0.33	19.09	95.23	17.29	0.0001
10000.	5.00	20.67	-0.30	20.97	124.23	19.16	0.0001
11000.	4.77	22.59	-0.27	22.86	158.76	21.05	0.0001
12000.	4.56	24.50	-0.25	24.74	199.31	22.93	0.0001
13000.	4.39	26.41	-0.23	26.63	246.37	24.82	0.0001
14000.	4.23	28.32	-0.21	28.53	300.44	26.71	0.0001
15000.	4.08	30.22	-0.19	30.42	362.01	28.60	0.0001
16000.	3.95	32.13	-0.18	32.31	431.58	30.49	0.0001
17000.	3.83	34.03	-0.17	34.21	509.64	32.38	0.0001
18000.	3.73	35.94	-0.16	36.10	596.68	34.27	0.0001
19000.	3.63	37.84	-0.15	38.00	693.20	36.17	0.0001
20000.	3.54	39.75	-0.14	39.89	799.70	38.06	0.0001

THE ABOVE RESULTS ARE FOR AN EXCITATION OF NI = 500. AMP/TURNS

Table 15 Sample data and results for low magnification conditions)

1000. 1000. 20 1 -200.

OBJECTIVE PROPERTIES OF  
POLE-PIECES OF FIG. 18B  
FOR LOW MAGNIFICATION CONDITIONS

(THE ABERRATION COEFFICIENTS ARE REFERRED TO THE IMAGE SIDE)

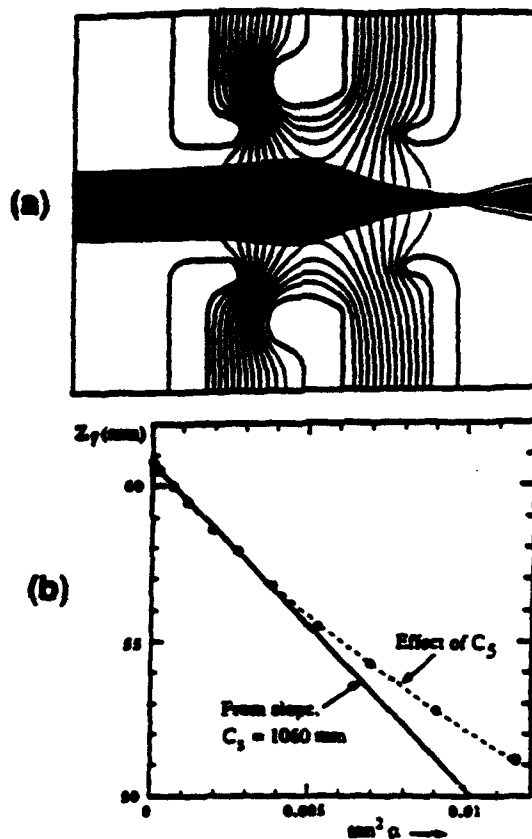
RC BEAM VOLTAGE	EXCITATION PARAMETER	OBJECT PLANE	IMAGE PLANE	MAG.	SPHER. AB.	CHROM. AB.	FIELD AT ZI
VR(VOLTS)	NI/SQRT(VR)	ZO(MM)	ZI(MM)	M	CSI(MM)	CCI(MM)	(TESLAS)
1000.	15.81	-200.00	1.99	0.023	3.20	3.45	0.0492
2000.	11.18	-200.00	4.87	0.032	6.10	5.06	0.0324
3000.	9.13	-200.00	7.25	0.042	10.79	6.85	0.0147
4000.	7.91	-200.00	9.50	0.051	18.34	8.87	0.0058
5000.	7.07	-200.00	11.71	0.061	29.73	11.05	0.0022
6000.	6.45	-200.00	13.92	0.072	46.03	13.37	0.0008
7000.	5.98	-200.00	16.17	0.083	68.46	15.82	0.0003
8000.	5.59	-200.00	18.45	0.094	98.43	18.37	0.0001
9000.	5.27	-200.00	20.76	0.105	137.55	21.05	0.0001
10000.	5.00	-200.00	23.12	0.117	187.64	23.84	0.0001
11000.	4.77	-200.00	25.53	0.129	250.78	26.75	0.0001
12000.	4.56	-200.00	27.99	0.141	329.31	29.78	0.0001
13000.	4.39	-200.00	30.50	0.153	425.90	32.94	0.0001
14000.	4.23	-200.00	33.06	0.166	543.55	36.25	0.0001
15000.	4.08	-200.00	35.67	0.179	685.67	39.69	0.0001
16000.	3.95	-200.00	38.35	0.192	856.09	43.28	0.0001
17000.	3.83	-200.00	41.08	0.206	1059.17	47.03	0.0000
18000.	3.73	-200.00	43.88	0.220	1299.78	50.94	0.0000
19000.	3.63	-200.00	46.75	0.234	1583.48	55.03	0.0000
20000.	3.54	-200.00	49.68	0.249	1916.48	59.29	0.0000

THE ABOVE RESULTS ARE FOR AN EXCITATION OF NI = 500. AMPTURNS

As noted in the Introduction, the above technique of Taylor series expansion only handles third order effects and this may result in poor accuracy for many situations. While the theory can be extended to higher orders, the resulting equations are much more complicated so that an alternative technique is necessary. One such alternative method of lens modeling is to give the lens design parameters (e.g. electrode shapes and potentials) to a program which determines the fields *everywhere* in the lens. Direct ray tracing can then be used to see how the electrons travel. This easily yields characteristics such as optimal focal plane position and focal spot size with high accuracy. The fields are determined by first solving for the potential, typically by either the FDM or FEM mesh methods. A recent innovation is the use of the ICCG method for solving the associated matrix equation for FEM determination of the potential; see Lencova and Lenc [11]. Lencova and Wisselink [31] also introduced automeshing capabilities for their lens design program - although there is a less serious need for this capability in lens design as compared to source modeling. Any good program for designing magnetic lenses should have the capability of handling magnetic saturation effects.

A commercial software package which is capable of modeling charged particle lenses using this second technique of direct ray tracing is the program OPTICS put out by Munro's company [20]. A typical example of the capability of Munro's software is shown in the top picture, (a), on the next page. The near vertical lines are the equipotentials between the two electrodes. The near horizontal lines are trajectories for electrons with different starting heights. The focal plane and spot size are easily determined from where the trajectories are most closely crossed together. A plot of focal position vs. square of ray slope is on the bottom - note the fifth order effect which the above third order theory would miss.

Examples of earlier work in computer modeling of electrostatic lenses may be found in the program CIELAS by Hill and Smith [32] and the program ELOP-GELOP by van Oostrum [33].



C. 1. Analysis of an electrostatic lens. (a) Equipotentials and trajectories computed using a finite difference program. (b) Plot of focal plane  $z_f$  vs  $\tan^2 \alpha$ , showing effect of primary spherical aberration  $C_3$  and fifth-order spherical aberration  $C_5$ .

## Deflector Modeling

Deflector modeling is similar to lens modeling in that one wants to determine the field distribution caused by electrode or current coil arrangements and then use electron ray tracing or aberration coefficients to predict the performance. The main difference between deflectors and lenses is that deflectors never have cylindrical symmetry, so determining the field distribution is a 3D problem. In principal, one could use, say, a 3D FEM program to solve for the fields. In practice, 3D models are so much more demanding of computer time and memory capacity compared to 2D models that they have not yet been used for deflector design. Instead, approximate methods have been developed to cope with the 3D problem.

It turns out that electrostatic deflectors, while lacking cylindrical symmetry, typically still possess some degree of axial rotation symmetry. In particular, the most common electrostatic deflectors have invariance with respect to rotations of either 90 or 45 degrees. In such a case, the 3D field distribution can be calculated via Fourier expansion as a sum of harmonic terms:

$$\begin{aligned}\Phi(r, \theta, z) &= \Phi_1(r, z)\cos(\theta) + \Phi_3(r, z)\cos(3\theta) + \dots \\ &= \left[ -f_1(z)r + \frac{1}{8}f_1''(z)r^3 \right]\cos(\theta) - f_3(z)r^3\cos(3\theta) + \dots\end{aligned}\quad (11)$$

(the rotational symmetry eliminates all even harmonic terms). The common approximation is to neglect the higher order terms and only deal with terms shown in the equation above; this may be an inadequate approach for large angle deflectors. Methods for calculating either the functions  $\Phi_m$  or the functions  $f_1$  and  $f_3$  for both magnetic and electrostatic deflectors are outlined in Munro and Chu [34]. These methods include invoking the Biot-Savart law for magnetic deflectors if no ferromagnetic materials are present - otherwise a FEM code is run. Likewise, electrostatic deflectors can be solved either by the BEM method or FEM. Lencova [35] reports a code for handling tapered magnetic deflectors.

There are many lenses, such as multipole lenses, slit lenses, grid lenses, and concentric hemispherical analysers which are not cylindrically symmetric. Multipole lenses, which are known to be capable of correcting beam aberrations [36], can be modeled exactly like deflectors if they have the same symmetry properties; Smith and Munro report a multipole/deflector program [37]. The other types of lenses may be modeled in a manner similar to equation (11), except that the lack of symmetry will mean that the even harmonic terms will need to be included.

Future trends for deflector modeling will probably be to increase the accuracy of the field calculations and to model traveling wave deflectors.

## Tolerances

A vital tool for charged particle optics design is a program which can calculate tolerances - the maximum amount of mechanical imperfections which do not move the performance out of specification. Typical imperfections are things like errors in machining or lens elements not being properly aligned.

The basis for all tolerance modeling programs is Sturrock's Principle [38]. Sturrock's Principle says that the effect of moving a point P on an electrode by the vector  $\delta \mathbf{r}_p$  is equivalent to leaving the point unchanged but changing the potential by  $\delta \Phi_p = - \nabla \Phi_p \cdot \delta \mathbf{r}_p$ . This is really convenient: to model the effect of, say, a lens being machined elliptical instead of cylindrical, one could actually model the lens as being cylindrical but now have a changed boundary potential (via Sturrock's principle). The fact that the boundary potential is no longer cylindrically symmetric means that the same techniques developed for deflector design must now be invoked, namely Fourier expansion as a sum of harmonic terms. Note that unlike deflector design, the even harmonic terms may be nonzero. This will now give you an approximation for the axial potential  $\Phi(r = 0, z)$  which, when combined with a unified lens/deflector aberration theory [7], allows you to compute the aberrations by numerically solving integrals.

Liu [39] and the references they cite describe a modern approach to lens and deflector tolerancing software. Archard [40] is a useful reference to assist in understanding Sturrock's original paper.

## Space Charge Modeling

All charged particle optical systems suffer from space charge effects. This refers to the mutually repulsive electric forces that similarly charged particles exert on each other [41]. Hence, a beam of electrons will actually have different trajectories when going through a lens than those that would be predicted from ray tracing when only the static fields from the lens are taken into account. These mutually repulsive forces have deleterious effects; the axial components cause the beam energy spread to widen (the "Boersch effect") and the radial components cause spatial broadening; both degrade the focusing ability of the system.

With an estimate for the beam current density, a first order model for the effects of space charge is to assume that the charge density is static and continuously distributed over the column and then to solve for the new fields in the system. For instance, to model space charge effects in an electrostatic lens in this manner, one would be solving Poisson's equation instead of the simpler Laplace's equation (which is used when only electrodes are considered). Fortunately, this only requires slight modification of the codes used in lens design.

One way to obtain an estimate for the current density is to calculate the fields with no charge assumed present, trace the trajectories of a bunch of particles through this system (where the particles start out with random positions, energies, and entry times - the randomness is a distribution obtained from some model), and then to use these trajectories to estimate the charge density. Now one can solve Poisson's equation for a more accurate solution. One could continue to iterate on the charge densities derived from successive solutions if desired. This is the method used by Munro in his electron gun program to simulate space charge effects near the source. He has found that this method converges to a solution in about 10 iterations (see p. 1866 of reference [12]).

A more effective method to model space charge is by full Monte Carlo simulation. In such a simulation, particles again are assigned random starting positions, energies, and entry times according to some distribution model. Then direct ray tracing is performed, using both the static fields from the optical elements and the dynamic electric fields generated by all the pair interactions. This method is appealing because it correlates with what is happening physically as a particle beam moves down a column. There are effects predicted by these Monte Carlo studies which the above first order models do not account for. In particular, when two real electrons make a close approach they experience higher angle scattering than the scattering predicted from a continuum distribution. This effect is known as residual stochastic Coulomb interactions. See Hawkes' book [42] for a brief discussion.

Numerically, there are two issues to be faced when implementing a Monte Carlo simulation. First, if there are  $N$  charged particles in the column, then the number of pair interactions which must be calculated grows as  $N^2$ . This makes a full Monte Carlo simulation of space charge effects computationally expensive when many particles are present (e.g. at high current levels). Unfortunately, this is precisely when you are most concerned about space charge effects. Second, the accuracy of the numerical ray tracing method is highly dependant upon choosing small time steps when two particles move close to each other. So, an appropriate algorithm must be employed to dynamically adjust the time step. This is additional overhead and the smaller time steps required also slow the program down. Other than these two considerations, a space charge modeling program is easy to implement as the electric field from pairwise interaction of electrons is trivial to calculate (the electrostatic expression is  $E = e \hat{r} / (4\pi\epsilon_0 r^2)$ ).

In spite of the computational expense involved in a full Monte Carlo simulation, many people have developed codes employing it. Munro's program COULOMB uses it [43]; his program can model Gaussian round-

beam and square-shaped beam systems and the column may contain include thin lenses, drift spaces, and uniform accelerating or retarding sections. Shimoyama [44] has apparently done a full Monte Carlo investigation into space charge effects in electron sources. Groves [45] and Sasaki [46] are among others who report full Monte Carlo simulation codes.

In order to speed up space charge calculations while keeping some of the benefits of a full Monte Carlo code (e.g. the hard scattering effects), there have been several attempts at approximate Monte Carlo methods. One approach is that of Allee [47], in which they restrict the number of pair interactions. Earlier work by Yau [48] had investigated the possibility of having a fixed sphere of influence about each electron such that only nearest neighbor interactions are considered. Allee incorporated a more sophisticated approach in which the size of this sphere (actually a cube) is dynamically adjusted so that on average only a specified number of electrons are inside it. The dynamic "sphere" adjustment is cleverly implemented so that only a few comparisons per electron need be done. They found that using only about 10 nearest neighbors gave results comparable to including all the pair interactions. As a result of considering fewer interactions, the calculation time will grow as  $N^{1.4}$ , which is superior to the  $N^2$  growth for a full Monte Carlo simulation.

Another possibility is the "Fast" Monte Carlo technique developed by Jansen [49], [50]. In this method, the particles are given random initial positions and velocities just as in a full Monte Carlo simulation. The difference is that the ray tracing is not done numerically but analytically: if one can assume that space charge interactions only cause small deviations in trajectory, then analytic formulas can be derived to calculate these deviations. These formulas may still require numerical methods to solve, but this turns out to be much quicker than numerical ray tracing. Jansen claims a speedup factor of 10 to 100 times for his method. The assumption about small deviations is not valid for all beam conditions - in particular, it becomes false for large beam currents. Nevertheless, for small to medium beam currents, his method may provide the fastest way to get a good estimate for space charge effects.

Special mention should be made here about space charge modeling for focused ion beam (FIB) systems. FIB's are more prone to suffer from space charge effects than electron systems for two reasons. First, ions are many thousands of times heavier than electrons, so for a given energy they move much slower. This means that to achieve a given beam current, the density of ions must be much greater than the density of electrons in a beam with the same current. Second, FIB's are typically operated at higher current levels than electron beams. Another way to recognize the susceptibility of FIB systems to space charge is the fact that a tightly focused charged particle beam is not in equilibrium, so the longer time of flight means greater relaxation towards equilibrium; see [42] and [50]. Two workers who report on Monte Carlo codes for FIB systems are Narum [51] and Vijgen [52]. Narum's code was capable of implementing a dynamic sphere of influence to limit the number of particle interactions and dynamic time steps while Vijgen's modeling used Jansen's "Fast" Monte Carlo programs.

Many of the issues discussed above may be found in greater detail in the recent excellent book by Jansen [53]. Additional references to Monte Carlo studies of Coulomb interactions may be found in [54].

## **Beam-Target Interactions**

Understanding beam-target interactions is very important for electron microscopy and electron/ion beam lithography. For example, to quantify images or understand charging effects in a Scanning Electron Microscope (SEM) will require detailed knowledge of the emission of secondary electrons [55]. Modeling beam-target interactions may be very important for lithographic applications where different parameters such as beam energy may greatly affect proximity exposure or sample damage.

An introduction to the physics of electron scattering and diffusion in solids can be found in Reimer [56]. David C. Joy has published an excellent introduction to Monte Carlo electron scattering simulations [57]. The typical method makes several simplifying assumptions. First, it is assumed that elastic scattering can be separated from inelastic scattering; elastic scattering is assumed responsible for changing the direction of the electron trajectory while inelastic scattering is assumed to only cause energy loss. Next, for elastic scattering, the solid lattice of atoms is viewed as a collection of the individual atoms. Finally, the inelastic scattering is assumed to continuously drain an electron of its energy at a rate given by the Bethe formula [58]. The elastic scattering cross section used is the screened Rutherford formula for an isolated atom; this formula predicts a mean free path which is used to determine in a random fashion how long an electron will travel until it next scatters. At its next scattering site, the scatter angle will next be determined and the whole process will be repeated until the electron runs out of energy due to the continuous inelastic scattering taking place between elastic scattering events. Several thousand computed trajectories will yield an estimate with a few percent error of such characteristics as electron penetration distance and energy deposition. Joy has made his programs freely available to the public [59].

One big weakness of this approach is the use of the screened Rutherford elastic cross section formula. It is known that this formula has limited validity - in particular, it is bad for elastic scattering off of heavy elements at low energies (below, say, 10 keV). A more accurate method of obtaining the elastic cross section is partial wave expansion using the Mott scattering formula, but this method requires an extensive calculation (several hours of supercomputer time) each time you want to use it [60]. Browning [61] has determined an empirical expression which interpolates over tabulated Mott cross section data for a large range of electron energies and atomic sizes. This now allows the significantly more accurate Mott cross sections to be used in a practical manner for Monte Carlo scattering simulations.

A more difficult area to accurately model is inelastic scattering. There are several important inelastic scattering mechanisms like atomic inner shell ionization (X-ray and Auger electron generation; see [62]), scattering from both valence and conduction electrons, and collective phenomena such as plasmon excitations. These effects may depend not only on atomic constituents, but also on crystal structure. There is a lack of accurate experimental data in this field. David Joy has compiled a database containing all the published data he could find on electron backscatter coefficients, secondary electron yield, stopping power, and X-ray ionization cross-sections [63]. A glance at the data reveals rather astonishing discrepancies between the results reported by different authors and large gaps between data points for many elements. The experiments done to gather this data are particularly difficult because the experimental apparatus is effectively part of the sample; no one has yet done a complete analysis of how to subtract this effect out [64]. As a result of this, it is not at all uncommon to see researchers publish papers in which, say, the forward and back scattered currents do not add up to 100% of the incident beam. In addition, the experimentalists have been irresponsible by not fully reporting the sample characteristics. For example, it might make a big difference in the data whether a carbon sample is amorphous, graphite, or diamond. The topography of the sample also has a large effect on, say, secondary electron yield (trenches will act as Faraday cups) yet this is another characteristic that may go unreported [64].

References to earlier work on Monte Carlo studies of electron scattering in solids may be found in [65]; references which focus on electron scattering as applied to electron beam lithography may be found in [66].

There is also interest in ion scattering in solids. People have done Monte Carlo studies of ion scattering in solids, but the problem is much more challenging than electron scattering. The reasons for this include atom knock-out effects (lattice atoms may get knocked out of their sites and in turn knock out other atoms causing a cascade effect), crystal effects like channeling (ions may travel further along certain crystal orientations), and the fact that a heavy enough ion dose will modify the characteristics of the sample (i.e. turn it amorphous). The people who are concerned with modeling ion scattering in solids appear to be mainly interested in ion implantation processes for the semiconductor industry; see the references in [67] for more details.

## Future directions

As this paper has shown, existing programs model many topics in charged particle systems. However, almost all of these programs exist in isolation so that one big feature would be the concatenation of many of the existing programs into one easy to use program. For instance, while there are programs to handle space charge effects, they are totally separate from those programs used in lens or deflector design while in reality you may want

to include space charge effects in the lens design stage. There is no one program which completely models an electron beam system from source all the way through optical elements and finally sample interaction.

An area that current computer modeling falls short in is optimization tools. Ideally, one should give an approximate lens design to the computer and the computer would then carry out a search through parameter space to try and find a more optimal solution. At present, such software is limited. Munro has put out the programs LITHO [68] and STIG [20], which performs optimization of stigmator and focusing systems, but the optimization is limited to those parameters like electrode potentials and coil currents which do not require new field calculations. Other researchers have investigated geometrical variations in the lenses, but they use many approximations to evaluate lens performance. Typical is van der Steen *et al* [69], Szilagyi and Szep [70], and Lenz [71] who solve for the axial potential of a cylindrically symmetric lens using various approximations and then use the paraxial ray equation for calculating trajectories. Kato and Tsuno [72] have attempted an optimization which modifies the geometrical shape of the lens, but they limited their optimization to minimizing the spherical aberration coefficient. Vertes *et al* [73] discuss lens optimization for analytical instruments (e.g. mass spectrometry); other work may be found in Olson and Kusse [74], and Rayces and Lebach [75]. The most difficult obstacle to overcome in finding a global optimization is the prodigious amount of computing power required. One algorithm which has become popular for solving multi-dimensional optimization problems is the simulated annealing algorithm; Forbes and Jones [76] discuss this method as applied to lens optimization.

Lastly, although automated mesh generation programs exist (e.g. the program SOGUN), they are typically not fully autonomous. Instead, the user (who will have insight into the problem to be solved) must still instruct the program where to put the heaviest concentration of grid lines. This may still be a tedious process. Furthermore, there is probably always a need for more sophisticated numerical methods to get ever more accurate field calculations. One technique that may relieve the user from guiding the mesh program while also being an accurate potential solver is the use of adaptive grids. To illustrate, suppose you allow the computer to autonomously set up a coarse, uniformly spaced grid and run an FEM code once to obtain a preliminary answer for the potentials. The computer could look to find where the equipotential lines lie in this first solution and then completely readjust the grid so that now the grid lines conform to the equipotential lines. This would automatically solve the problem of ensuring that enough grid elements are present where the field is rapidly changing. A few iterations should converge to an extremely accurate answer. Furthermore, there may be fundamental numerical accuracy benefits or new algorithms that can be exploited if the grid lines are on approximate equipotentials.

## Acknowledgements

We would like to acknowledge our debt to the recent review paper by Munro given below, which helped immensely in the preparation of this document - Figures 1, 7, and 8 are courtesy of this paper. The book by Hawkes and Kasper was very helpful. We also greatly appreciate the conversations with Ray Browning who shared his expertise in many areas of electron beams.

This work was supported by ONR grant # N00014-92-J-1996.

P. W. Hawkes and E. Kasper, *"Principles of Electron Optics"*, Academic Press (1989)  
Vol. 1 & 2.

E. Munro, *"Numerical modeling of electron and ion optics on personal computers"*,  
J. Vac. Sci. Technol. B 8 (6), Nov/Dec 1990 pp. 1657-1665.

## References

- [1] G. Liebmman *et al.*, "Solution of Partial Differential Equations with a Resistance Network Analogue", Br. J. Appl. Phys., April 1950, pp. 92-103.
- G. Liebmman *et al.*, "The Symmetrical Magnetic Electron Microscope Objective Lens with Lowest Spherical Aberration", Proc. Phys. Soc. London Sect. B, Vol. 64, No. 383, 1951, pp. 972-977.
- G. Liebmman *et al.*, "The Magnetic Electron Microscope Objective Lens of Lowest Chromatic Aberration", Proc. Phys. Soc. London Sect. B, Vol. 65, No. 357, 1952, pp. 188-192.
- [2] E. Munro, in *Proceedings of the 7th International Congress on Electron Microscopy, Grenoble, September 1970* (Societe Francaise de Microscopie Electronique, Paris, 1970), Vol. 2, p. 55.
- [3] H. C. Pfeiffer, "Basic limitations of probe forming systems due to electron-electron interaction", Proceedings of the 5th annual scanning electron microscope symposium part I and part II, workshop on biological specimen preparation for scanning electron microscopy, pp. 113-120; held 25-27 April 1972 Chicago, IL, USA; published by IIT Research Institute, Chicago, IL, USA (editors: O. Johari and I. Corvin).
- [4] T. Groves, D. L. Hammond, H. Kuo, "Electron-beam broadening effects caused by discreteness of space charge effects", J. Vac. Sci. Technol., Vol. 16, No. 6, November 1979, pp. 1680-1685.
- [5] M. E. Haine and P. A. Einstein, "Characteristics of the Hot Cathode Electron Microscope Gun", Br. J. Appl. Phys., February 1952, pp. 40-46.
- M. E. Haine, P. A. Einstein, and P. H. Brocherd, "Resistance Bias Characteristic of the Electron Microscope Gun", Br. J. Appl. Phys., Vol. 9, No. 12, 1958, pp. 482-486.
- [6] A. B. El-Kareh and J. C. J. El-Kareh, "Electron Beams, Lenses, and Optics", Academic Press, New York (1970) Vol. 1, p. 249.
- P. W. Hawkes and E. Kasper, "Principles of Electron Optics", Academic Press (1989), Vol. 1, pp. 85-87.
- [7] H. C. Chu and E. Munro, "Numerical analysis of electron beam lithography systems. Part III: Calculation of the optical properties of electron focusing systems and dual-channel deflection systems with combined magnetic and electrostatic fields", Optik, 61, No. 2 (1982), pp. 121-145.

P. W. Hawkes and E. Kasper, *"Principles of Electron Optics"*, Academic Press (1989),  
Vol. 1, Chapter 24.

[8] A. Renau, F. H. Read, and J. N. H. Brunt, *"The charge-density method of solving electrostatic problems with and without the inclusion of space-charge"*, J. Phys. E: Sci. Instrum., Vol. 15 (1982), pp. 347-354.

E. Munro and H. C. Chu, *"Numerical analysis of electron beam lithography systems. Part II: Computation of fields in electrostatic deflectors"*, Optik, 61, No. 1 (1982), pp. 3-5.

P. W. Hawkes and E. Kasper, *"Principles of Electron Optics"*, Academic Press (1989),  
Vol. 1, pp. 125-158 (especially p.150).

H. A. Van Hoof, *"A new method for numerical calculation of potentials and trajectories in systems of cylindrical symmetry"*, J. Phys., E (London). Sci. Instrum. (Oct 1980). v. 13 (10) pp. 1081-1089.

[9] P. W. Hawkes and E. Kasper, *"Principles of Electron Optics"*, Academic Press (1989),  
Vol. 1, p. 175ff.

[10] J. A. Meijerink and H. A. Van der Vorst, Math. Comp. 31 (1977), p. 148.

[11] B. Lencova and M. Lenc, Optik 68 (1984), p. 37.

B. Lencova and M. Lenc, in *Scanning Electron Microscopy 1986*, edited by O. Johari (SEM Inc., AMF O'Hare, Chicago, IL, 1986), p. 897.

[12] Xieqing Zhu and Eric Munro, *"A computer program for electron gun design using second-order finite elements"*, J. Vac. Sci. Technol. B 7 (6), Nov/Dec 1989, p. 1862.

[13] Charles A. Hall and Thomas A. Porsching, *"Numerical Analysis of Partial Differential Equations"*, Prentice Hall, Englewood Cliffs NJ (1990).

[14] H. Magnin and J. L. Coulomb, *"Towards a distributed finite element package for electromagnetic field computation"*, IEEE Transactions on Magnetics (March 1993) vol.29, no.2, pp. 1923-6.

T. Yamabuchi, S. Fujii, T. Murai, S. Hirose, T. Futagami, Y. Kagawa, *"Finite element analysis of electromagnetic field via three-dimensional hexagonal edge elements"*, Electronics and Communications in Japan, Part 2 (Electronics) (Sept. 1992) vol.75, no.9, pp. 1-13.

T. Onuki, S. Wakao, *"Hybrid finite element and boundary element method utilizing scalar potential for 3D electromagnetic field analysis"*, Transactions of the Institute of Electrical Engineers of Japan, Part A (May 1992) vol.112-A, no.5, pp. 346-54.

L. Pichon and A. Razek, "Analysis of electromagnetic forces and mechanical behaviour in a tubular induction device with a hybrid FEM-BEM technique", *COMPEL - The International Journal for Computation and Mathematics in Electrical and Electronic Engineering* (March 1992) vol.11, no.1, pp. 169-72.

D. N. Ladd and G. I. Costache, "Computation of the electromagnetic field distribution inside enclosures with apertures using 3-D FEM", *International Journal of Numerical Modelling: Electronic Networks, Devices and Fields* (Sept. 1991) vol.4, no.3, pp. 175-88.

K. Tahir and T. Mulvey, "Pitfalls in the calculation of the field distribution of magnetic electron lenses by the finite-element method", *Nuclear Instruments & Methods in Physics Research, Section A (Accelerators, Spectrometers, Detectors and Associated Equipment)* (1 Dec. 1990) vol.A298, no.1-3, pp. 389-95.

P. R. Kotiuga, "Is three-dimensional electromagnetic field analysis incompatible with node-based finite element interpolation?", in *Advances in Electrical Engineering Software. Proceedings of the First International Conference on Electrical Engineering Analysis and Design*.

P. P. Silvester (editor), Southampton, UK: Comput. Mech. Publications, 1990. pp. 187-90.

Huang Ping, Jiang Zejia, Jiang Kexun, "A new approach for accurate calculation of electromagnetic field: low-order FEM for potential, high-order for field", *IEEE Transactions on Magnetics* (Sept. 1987) vol.MAG-23, no.5, pt.1, pp. 2668-70.

Liang Xuebiao, Jian Baidun, Ni Guangzhen, "The B-spline finite element method in electromagnetic field numerical analysis", *IEEE Transactions on Magnetics* (Sept. 1987) vol.MAG-23, no.5, pt.1, pp. 2641-3.

[15] M. D. Lunney and R. B. Moore, "The computation of electric fields for numerical integration of charged particle motion", *IEEE Transactions on Magnetics* (Sept. 1991) vol.27, no.5, pp. 4174-6.

[16] William H. Press, Saul A. Teukolsky, William T. Vetterling, and Brian P. Flannery, "Numerical Recipes in C The Art of Scientific Computing", Second Edition, 1992, Cambridge University Press, Chapter 16.

[17] M. D. N. Lunney, R. B. Moore, J. P. Webb, B. Forghani, "Particle trajectory calculations using finite element electromagnetic field maps", *IEEE Transactions on Magnetics* (Nov. 1988) vol.24, no.6, pp. 3126-8.

[18] E. J. Nystrom, "Uber die numerische Integration von Differential-gleichungen", *Acta Soc. sc. Fennicae*, Vol. 50, No. 13, 56 S., 1925.

Nguyen huu Cong, "Note on the performance of direct and indirect Runge-Kutta-Nystrom methods", *J. Comp. Appl. Math.*, Vol. 45, No. 3, 3 May 1993, pp. 347-355.

P. W. Sharp and J. M. Fine, "A contrast of direct and transformed Nystrom pairs", *J. Comp. Appl. Math.*, Vol. 42, No. 3, 30 October 1992, pp. 293-308.

P. W. Sharp and J. M. Fine, "Some Nystrom pairs for the general second-order initial-value problem", *J. Comp. Appl. Math.*, Vol. 42, No. 3, 30 October 1992, pp. 279-291.

- [19] NASA Tech Briefs, November 1993, pp. 102 & 106. Further information available upon request.
- [20] Here is the address to contact Munro's company for information about their programs:  
Munro's Electron Beam Software Ltd  
14 Cornwall Gardens, London SW7 4AN, England  
tel: 011 44 71 581 4479
- [21] E. Munro, private communication.
- [22] C. Weber, Philips Res. Reports (Suppl.) No.6 (1967).
- [23] W. B. Herrmannsfeldt, Electron Trajectory Program SLAC-226 (Stanford, CA) (1976).
- [24] N. K. Kang, J. Orloff, L. W. Swanson, and D. Tuggle, J. Vac. Sci. Technol. 19 (1981), p. 1077.
- [25] A. Renau, F. H. Read, and J. N. H. Brunt, J. Phys. E 15 (1982), p. 347.
- [26] The program EBEAM by R. Browning; as yet unpublished.
- [27] P. W. Hawkes and E. Kasper, "Principles of Electron Optics", Academic Press (1989) Vol. 2, pp. 953-970.
- [28] Z. Cui and L. Tong, J. Vac. Sci. Technol. B 6 (1988), p. 2104.
- [29] O.A. Mohammed and L. F. Garcia, "An optimum finite element automatic grid generator for electromagnetic field computations", IEEE Transactions on Magnetics (Nov. 1988) vol.24, no.6, pp. 3177-9.  
L.F. Garcia and O. A. Mohammed, "An automatic finite element grid generator for electromagnetic field computations", Miami Technicon '87. An International Conference (Cat. No.87TH0206-3). M.L Heimer and D.J. Larnard (editors) New York, NY, USA: IEEE, 1987. pp. 179-82.
- [30] This manual is apparently unpublished. It was provided to the Pease research group at Stanford University by Munro himself during a visit to the group. A reference that gives related material is:  
E. Munro, "Computer-aided design of electron lenses by the finite element method", p. 284-323 in "Image processing and computer-aided design in electron optics" edited by P. W. Hawkes, Academic Press, London, 1973.

- [31] B. Lencova and G. Wisselink, Nucl. Instrum. Methods Phys. Res. A **298** (1990), p. 56.
- [32] R. Hill and K. C. A. Smith, *Electron Microscopy and Analysis, 1981. Proceedings of EMAG 81*, Cambridge, 7-10 September, 1981 (Goringe, M. J., ed.; Institute of Physics, Bristol, 1982) Conference Series **61**, pp. 71-74.  
R. Hill and K. C. A. Smith, *Electron Microscopy 1980. Proceedings of the Seventh European Congress on Electron Microscopy, The Hague*, vol. 1, pp. 60-61.
- [33] K. J. van Oostrum, Philips Tech. Rev. **42** (1985), pp. 69-84.
- [34] E. Munro and H. C. Chu, Optik **60** (1981/82) p. 371.  
E. Munro and H. C. Chu, Optik **61**, No.1 (1982) p. 1.
- [35] B. Lencova, M. Lenc, and K. D. van der Mast, J. Vac. Sci. Technol. B **7** (1989), p. 1846.
- [36] O Scherzer, Optik **34** (1947), p. 114.
- [37] M. R. Smith and E. Munro, J. Vac. Sci. Technol. B **5** (1987), p. 161.  
M. R. Smith, Ph. D. dissertation, University of London, 1988.  
M. R. Smith and E. Munro, in the *International Symposium on Focused Ion Beam Technology at the 174th Meeting of Electrochemical Society, Chicago, 1988*, Extended Abstract No. 455 (Electrochemical Society, Princeton, NJ, 1988).
- [38] P. A. Sturrock, Philos. Trans. R. Soc. London, Ser. A **243** (1951), p. 387.
- [39] H Liu, X. Zhu, and E. Munro, J. Vac. Sci. Technol. B **8** (6), Nov/Dec 1990 pp. 1676-1681.
- [40] G. D. Archard, J. Sci. Inst. **30**, 1953, p. 353.
- [41] Actually, charged particles which move will also generate magnetic fields, although the forces from this are typically so small that these magnetic fields are ignored. Exception: there are relativistic effects when particles move at high speeds (e.g. a 100 keV electron). For details on this, one might consult D. J. Griffiths, *"Introduction to Electrodynamics"*, Prentice-Hall 1981, pp. 370-372 and pp. 439-444.
- [42] P. W. Hawkes and E. Kasper, *"Principles of Electron Optics"*, Academic Press (1989), Vol. 2, pp. 1004-1016.

[43] E. Munro, "Numerical modeling of electron and ion optics on personal computers", J. Vac. Sci. Technol. B 8 (6), Nov/Dec 1990 pp. 1659-1660.

[44] H. Shimoyama, Y. Shimazaki, and A. Tanaka, "Computer simulation of energetic Boersch effect in the diode region of the field emission gun", in Charged-Particle Optics, William B. Thompson, Mitsugu Sato, Albert V. Crewe, Editors, Proc. SPIE 2014, pp. 99-103. Unpublished at the time this review paper written.

[45] T. R. Groves, D. L. Hammond, and H. Kuo, J. Vac. Sci. Technol. 19 (1981), p. 1094.

[46] T. Sasaki, Conference on VLSI: Architecture, Design, and Fabrication, (California Institute of Technology, 1979); J. Vac. Sci. Technol. 21 (1982), p. 695.

[47] D. R. Allee, J. D. Pehoushek, R. F. W. Pease, "Novel Monte Carlo Simulation of Space Charge Effects in Laser Irradiated Thermionic and Photoemissive Electron Sources",  
32nd International Symposium on Electron, Ion, and Photon Beams  
Fort Lauderdale, FL, USA, 31 May - 3 June 1988.  
Published in J. Vac. Sci. Technol. B Nov/Dec 1988, vol. 6, no. 6, pp. 1989-94.

[48] Y. W. Yau, R. F. W. Pease, and T. R. Groves, J. Vac. Sci. Technol. B 1 (1983), p. 1141.

[49] G. H. Jansen, "Fast Monte Carlo simulation of charged particle beams", J. Vac. Sci. Technol. B 5 (1), Jan/Feb 1987, pp. 146-149.

[50] G. H. Jansen, "Advances in Electronics and Electron Physics", Academic Press  
1990 Suppl. 22.

[51] D. H. Narum and R. F. W. Pease, "New techniques for modeling focused ion beams",  
J. Vac. Sci. Technol. B 4 (1), Jan/Feb 1986, p. 154.

[52] L. J. Vijgen and P. Kruit, "Coulomb interactions in a shaped ion beam pattern generator", J. Vac. Sci. Technol. B 10 (6), Nov/Dec 1992, pp. 2809-2813.

[53] G. H. Jansen, "Coulomb Interactions in Particle Beams", Academic Press 1990.

[54] S. E. Kuhn and G. E. Dodge, "A fast algorithm for Monte Carlo simulations of multiple Coulomb scattering", Nuclear Instruments & Methods in Physics Research, Section A (Accelerators, Spectrometers, Detectors and Associated Equipment) (15 Oct. 1992) vol.A322, no.1, pp. 88-92.

V. Beck, M. Gordon, T. Groves, "A fast Monte Carlo beam simulator using exact Coulomb scattering", Journal of Vacuum Science & Technology B (Microelectronics Processing and Phenomena) (Nov.-Dec. 1989) vol.7, no.6, pp. 1438-42.

[55] D. C. Joy, "A model for calculating secondary and backscattered electron yields", J. Microscopy., Vol. 147, Pt. 1, July 1987, pp. 51-64.

H. Seiler, "Secondary electron emission in the scanning electron microscope", J. Appl. Phys. 54 (11) November 1983, pp. R1-R18.

[56] L. Reimer, "Scanning Electron Microscopy", (Springer-Verlag 1985), Chapter 3.

7] David C. Joy, "An Introduction to Monte Carlo simulations", EUREM 88, Vol. 1, pp. 24-32.  
(Proceedings from: 9th European Congress on Electron Microscopy (EUREM-9) and Exhibition, York (UK), 4-9 Sept. 1988. Institute of Physics conference series no. 93).

[58] The Bethe formula is  $\frac{dE}{dS} = -78500 \frac{\rho Z}{A E} \log\left(\frac{1.166E}{J}\right)$  (keV / cm). Joy has recently published a simple extension to this formula to more accurately model low energy electrons - see this reference:

D. C. Joy and S. Luo, "An Empirical Stopping Power Relationship for Low-Energy Electrons", SCANNING Vol. 11 (1989), pp. 176-180 (FACM Publishing Co., Inc.).

[59] David C. Joy may be contacted at either  
EM Facility, University of Tennessee  
Knoxville, TN 37996-0810

or

Oak Ridge National Laboratories  
Oak Ridge, TN 37831

[60] Z. Czyzewski, D. MacCallum, A. Romig, and D. C. Joy, "Calculations of Mott scattering cross section", J. Appl. Phys. 68 (7), 1 October 1990, pp. 3066-3072.

L. Reimer and B. Lodding, "Calculations and Tabulation of Mott Cross-Sections for Large-Angle Electron Scattering", SCANNING Vol.6, pp. 128-151 (1984) (FACM Publishing Co., Inc.).

M. E. Riley, C. J. MacCallum, F. Biggs, "Theoretical Electron-Atom Elastic Scattering Cross Sections", Atomic Data and Nuclear Data Tables, Vol. 15, No. 5, May 1975.

[61] R. Browning, T. Z. Li, B. Chui, Jun  $\nu$ , R. F. W. Pease, Z. Czyzewski, and D. C. Joy, "Empirical Forms for the Electron/Atom Elastic Scattering Cross Sections from 0.1-30 keV", submitted to the Journal of Applied Physics, 9/93.

R. Browning, "Universal elastic scattering cross sections for electrons in the range 1-100 keV", Appl. Phys. Lett. 58 (24), 17 June 1991, pp. 2845-2847.

[62] T. S. Rao-Sahib and D. B. Wittry, "X-ray continuum from thick elemental targets for 10-50 keV electrons", J. Appl. Phys. Vol. 45, No. 11, November 1974, pp. 5060-5068.

[63] David C. Joy, "A Data Base on Electron-Solid Interactions", as yet unpublished.  
Contact him at the address given in [59] for a copy.

[64] R. Browning, private communication.

[65] H. J. Fitting and J. Reinhardt, "Monte-Carlo Simulation of keV-Electron Scattering in Solid Targets", Phys. Stat. Sol. (a) 88 (1985), pp. 245-259.

N. Samoto and R. Shimizu, "Theoretical study of the ultimate resolution in electron beam lithography by Monte Carlo simulation, including secondary electron generation: Energy dissipation profile in polymethylmethacrylate", J. Appl. Phys., Vol. 54, No. 7, July 1983, pp. 3855-3859.

M. Kotera, K. Murata, and K. Nagami, "Monte Carlo simulation of 1-10-keV electron scattering in a gold target", J. Appl. Phys. 52 (2), February 1981, pp. 997-1003.

G. Love, M. G. Cox, and V. D. Scott, "A versatile atomic number correction for electron-probe microanalysis", J. Phys. D: Appl. Phys., Vol. 11, 1978, pp. 7-21.

[66] Kang-Yoon Lee, Guang-Sup Cho, Duk-In Choi, "Monte Carlo simulation of energy dissipation in electron beam lithography including secondary electron generation", Journal of Applied Physics (15 June 1990) vol.67, no.12, pp. 7560-7.

K. D. Cummings and D. J. Resnick, "A Monte Carlo simulation of electron beam lithography used to create 0.5-  $\mu$ m structures on GaAs", Journal of Vacuum Science & Technology B (Microelectronics Processing and Phenomena) (Nov.-Dec. 1988) vol.6, no.6, pp. 2033-6.

[67] M. D. J. Bowyer et al, "Central moments of ion implantation distributions derived by the backward Boltzmann equation compared with Monte Carlo simulations", J. of Phys. D (Applied Physics), vol. 25, no. 11, 14 Nov. 1992, pp. 1619-29.

K. M. Klein et al, "Monte Carlo simulation of ion implantation into single-crystal silicon including new models for electronic stopping and cumulative damage", International Electron Devices Meeting 1990. Technical Digest (Cat. No. 90CH2865-4). (USA: IEEE, 1990 pp. 745-8).

H. Nakano et al, "Monte Carlo simulation of ion-channeling spectra from partially damaged crystals", J. Appl. Phys., 1 Jan. 1992, vol. 71, no. 1, pp. 133-9.

G. R. Srinivasan et al, "Monte Carlo modeling of ion implantation for silicon devices", International Electron Devices Meeting 1989. Technical Digest (Cat. No. 89CH2637-7). (USA: IEEE, 1989 pp. 687-90).

T. L. Crandle et al, "Analysis of ion implant processes through Monte Carlo based simulation", Solid State Technology, Jan. 1990, vol. 33, no. 1, pp. 43-5.

[68] H. C. Chu and E. Munro, Optik 61 (1982) p. 213.

[69] H. W. G. van der Steen, J. E. Barth, and J. P. Adriaanse, "Engineering constraints and computer-aided optimization of electrostatic lens systems", Nuclear Instruments & Methods in Physics Research, Section A (1 Dec. 1990) vol.A298, no.1-3, pp. 377-82.

H. W. G. van der Steen and J. E. Barth, "Practical optimization of multielectrode lenses", Journal of Vacuum Science & Technology B (Nov.-Dec. 1989) vol.7, no.6, pp. 1886-90.

J. P. Adriaanse, H. W. G. van der Steen, and J. E. Barth, "Practical optimization of electrostatic lenses", Journal of Vacuum Science & Technology B (July-Aug. 1989) vol.7, no.4, pp. 651-66.

[70] M. Szilagyi and J. Szep, "Optimum design of electrostatic lenses", Journal of Vacuum Science & Technology B (May-June 1988) vol.6, no.3, pp. 953-7.

[71] F. Lenz, "Optimization of the imaging properties of an electron optical demagnifying system consisting of four magnetic lenses", Optik (1988) vol.78, no.4, pp. 135-40.

[72] M. Kato and K. Tsuno, "Optimization of electron lens shape giving minimum spherical aberration coefficient", IEEE Transactions on Magnetics (March 1990) vol.26, no.2, pp. 1023-6.

[73] A. Vertes, P. Juhasz, L. Balazs, M. De Wolf, and R. Gijbels, "Non-linear optimization of cylindrical electrostatic lenses", International Journal of Mass Spectrometry and Ion Processes (6 July 1988) vol.84, no.3, pp. 255-69.

[74] J. C. Olson and B. R. Kusse, "*First-order optimization of multiple magnetic lens systems for transport and focusing of annular ion beams*", Journal of Applied Physics (15 Nov. 1991) vol.70, no.10, pt.1, pp. 5179-85.

[75] J. L. Rayces and L. Lebach, "*RAY-CODE: an aberration coefficient oriented lens design and optimization program*", Proceedings of the SPIE - The International Society for Optical Engineering (1987) vol.766, pp. 230-45.

[76] G. Forbes and A. Jones, "*Global optimization in lens design*", Optics & Photonics News (March 1992) vol.3, no.3, pp. 22-6, 28-9.